

## SUPPLEMENTARY INFORMATION

### Thermal therapy Histology

Day 3 histology of the treated tumors revealed distinct histological zones concentric to the cryoprobe tract characteristic of cryosurgical lesions as reported previously (Figure S1A)<sup>1,2</sup>. A zone of central necrosis was present immediately adjacent to the cryoprobe tract and characterized by increased eosinophilic staining with necrotic tumor cells with absent or pyknotic nuclei and few scattered inflammatory cells. In the control and AuPEG groups the central necrotic zone was surrounded by a ~0.5-1mm band of inflammatory cells (mostly neutrophils) which in turn was surrounded by a thrombosis/ischemic necrosis zone and viable tumor tissue. In the NP-TNF group, the central necrosis zone was larger with almost no inflammatory cells. Additionally, the inflammatory band and the zone of thrombosis/ischemic necrosis were narrower and closer to the edge of viable tumor tissue. The histological stasis areas (defined by the boundary between the cryosurgical lesion and the edge of viable tumor tissue) obtained at Day 3 correlated well with the trend seen in the vascular stasis areas i.e. the histological stasis area of NP-TNF group was significantly larger than the control and AuPEG groups. The slight difference observed in the NP-TNF group between the Day 3 histology and vascular stasis areas was not statistically significant ( $p = 0.31$ ).

Day 3 histology of the HTT treated tumors revealed distinct histological zones concentric to the probe tract characteristic of thermal lesions as reported previously (Figure S1B)<sup>3-5</sup>. The histologic zones were similar to those seen after cryosurgery with some marked differences. The tissue within the central necrotic zone immediately adjacent to the probe tract appeared

“thermally fixed” with architectural and cytologic preservation similar to that seen after formalin fixation. Also, the central necrotic zone had less intense eosinophilic staining compared to cryosurgical lesions and more nuclear staining. The edge of the thermal lesion was in general less circular with more jagged edges compared to the cryosurgical lesions obtained. The histological stasis area obtained at Day 3 was significantly lower than the vascular stasis area for the NP-TNF group ( $p < 0.01$ ). However, there was no statistically significant difference between the control and AuPEG groups’ histological and vascular stasis areas.

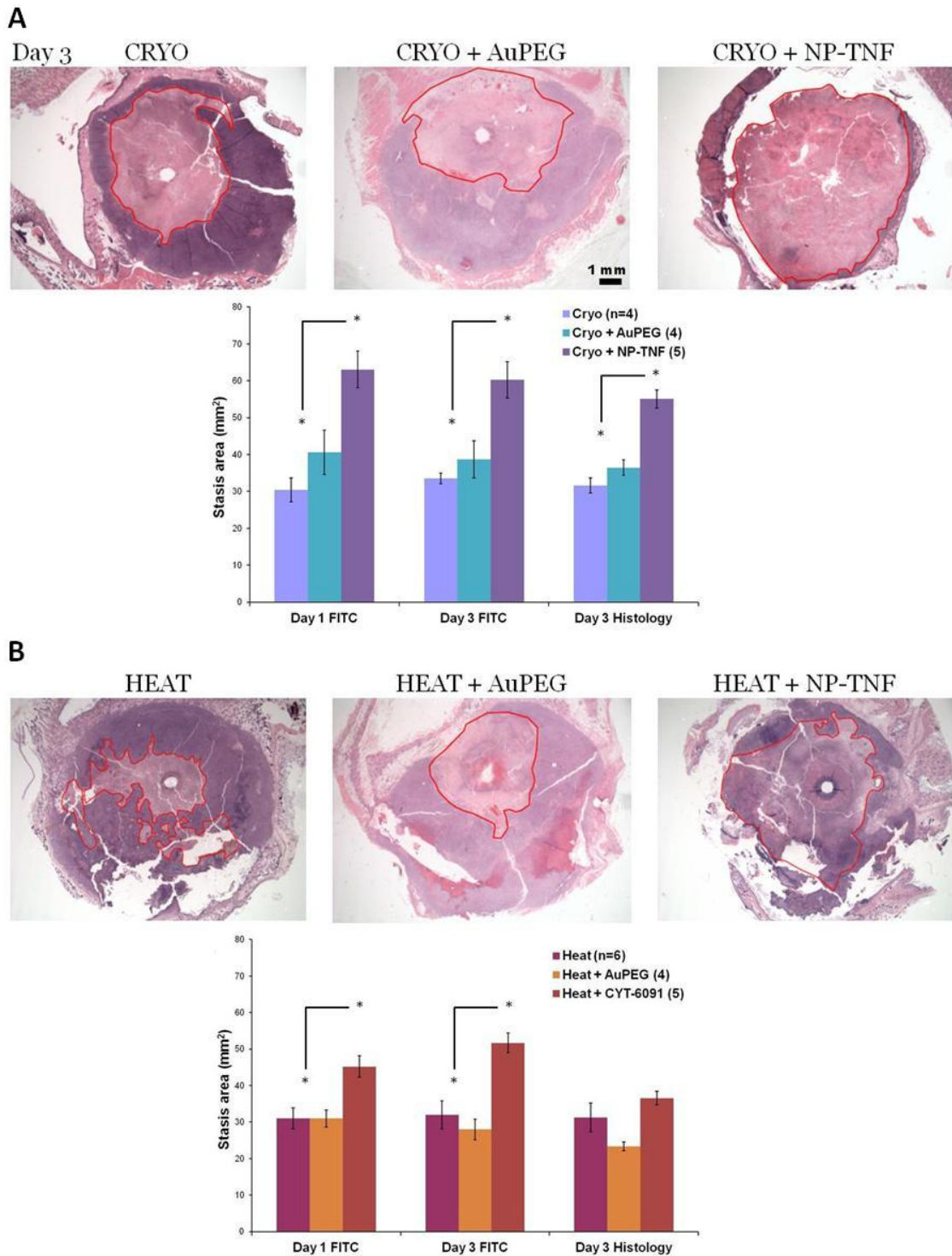


**Figure S1.** NP preconditioning enhances thermal injury in DSFC LNCaP tumors. Representative H&E stained sections of entire DSFC tumors at Day 3 after (A) cryosurgical and (B) high temperature thermal treatment with or without nanoparticle pretreatment. Histological stasis areas are outlined in red in each section. Graphs depict vascular and histological stasis area measurements for each thermal therapy (\*,  $p < 0.05$ ). Data presented as mean  $\pm$  SE.

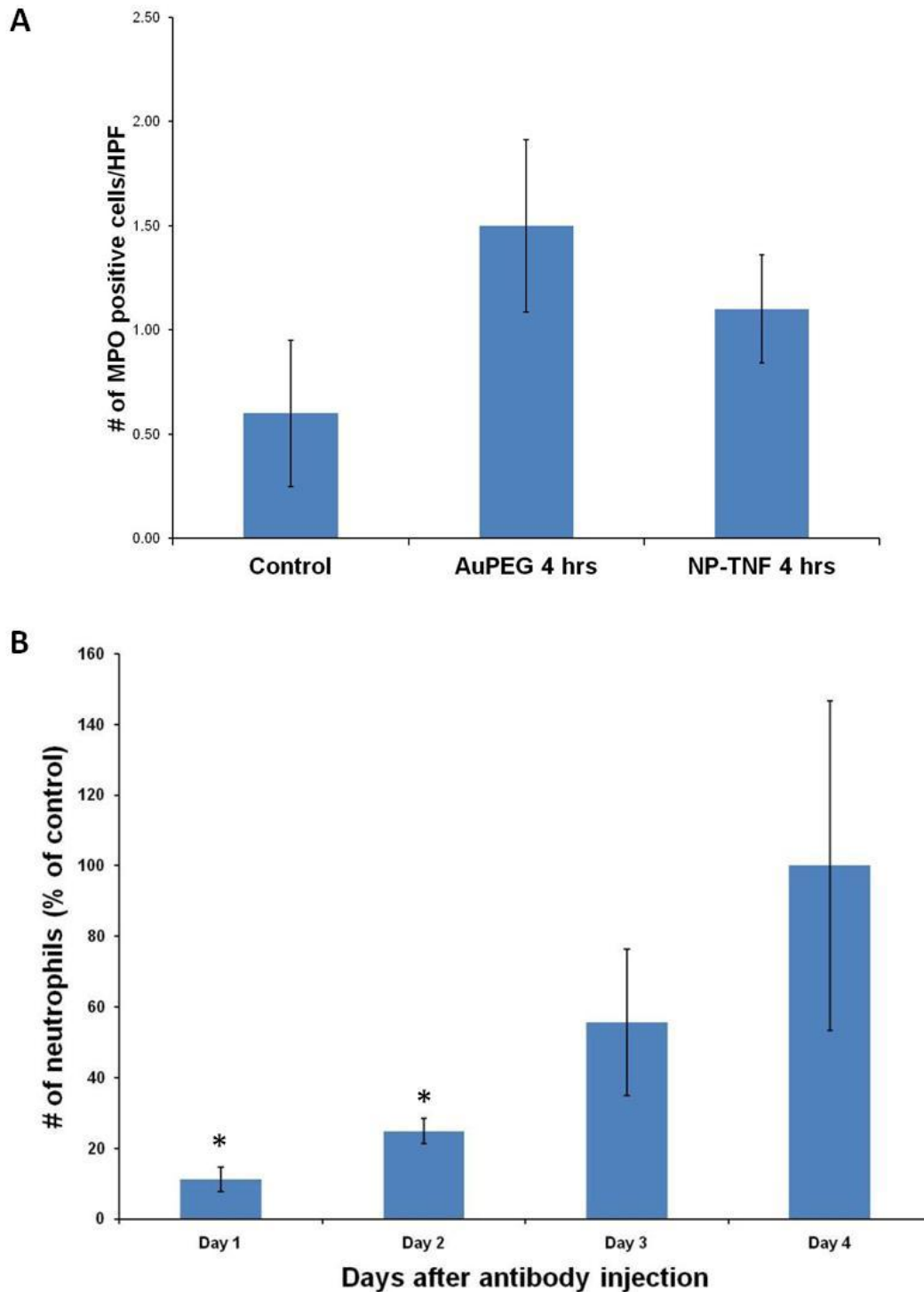


**Figure S2.** (A) High field power count of myeloperoxidase (MPO) positive cells i.e. neutrophils in DSFC LNCaP tumors 4 hours after NP-TNF systemic administration. There were no statistically significant differences between the 3 groups. (B) Circulating neutrophil number obtained from serial blood draws over 4 days after i.p. injection of Anti-Ly6G Ab demonstrates systemic depletion of neutrophils at 24 hrs (\*,  $p < 0.05$  compared to control).

## REFERENCES

1. Chao, B. H.; He, X.; Bischof, J. C. Pre-treatment inflammation induced by TNF-alpha augments cryosurgical injury on human prostate cancer. *Cryobiology* **2004**, *49*, (1), 10-27.
2. Jiang, J.; Goel, R.; Schmechel, S.; Vercellotti, G.; Forster, C.; Bischof, J. Pre-Conditioning Cryosurgery: Cellular and Molecular Mechanisms and Dynamics of TNF-alpha Enhanced Cryotherapy in an in vivo Prostate Cancer Model System. *Cryobiology* **2010**.
3. Bhowmick, S.; Hoffmann, N. E.; Bischof, J. C. Thermal therapy of prostate tumor tissue in the dorsal skin flap chamber. *Microvasc Res* **2002**, *64*, (1), 170-3.
4. Bhowmick, S.; Swanlund, D. J.; Coad, J. E.; Lulloff, L.; Hoey, M. F.; Bischof, J. C. Evaluation of thermal therapy in a prostate cancer model using a wet electrode radiofrequency probe. *J Endourol* **2001**, *15*, (6), 629-40.
5. He, X.; McGee, S.; Coad, J. E.; Schmidlin, F.; Iaizzo, P. A.; Swanlund, D. J.; Kluge, S.; Rudie, E.; Bischof, J. C. Investigation of the thermal and tissue injury behaviour in microwave thermal therapy using a porcine kidney model. *Int J Hyperthermia* **2004**, *20*, (6), 567-93.